PTP and LTP at a hippocampal mossy fiber-interneuron synapse

Henrik Alle, Peter Jonas, and Jörg R. P. Geiger*

Physiologisches Institut der Universität Freiburg, D-79104 Freiburg, Germany

Edited by Roger A. Nicoll, University of California, San Francisco, CA, and approved September 27, 2001 (received for review December 22, 2000)

The mossy fiber-CA3 pyramidal neuron synapse is a main component of the hippocampal trisynaptic circuitry. Recent studies, however, suggested that inhibitory interneurons are the major targets of the mossy fiber system. To study the regulation of mossy fiber-interneuron excitation, we examined unitary and compound excitatory postsynaptic currents in dentate gyrus basket cells, evoked by paired recording between granule and basket cells or extracellular stimulation of mossy fiber collaterals. The application of an associative high-frequency stimulation paradigm induced posttetanic potentiation (PTP) followed by homosynaptic long-term potentiation (LTP). Analysis of numbers of failures, coefficient of variation, and paired-pulse modulation indicated that both PTP and LTP were expressed presynaptically. The Ca^{2+} chelator 1,2-bis(2-aminophenoxy)ethane-*N*,*N*,*N*′,*N*′-tetraacetic acid (BAPTA) did not affect PTP or LTP at a concentration of 10 mM but attenuated LTP at a concentration of 30 mM. Both forskolin, an adenylyl cyclase activator, and phorbolester diacetate, a protein kinase C stimulator, lead to a long-lasting increase in excitatory postsynaptic current amplitude. H-89, a protein kinase A inhibitor, and bisindolylmaleimide, a protein kinase C antagonist, reduced PTP, whereas only bisindolylmaleimide reduced LTP. These results may suggest a differential contribution of protein kinase A and C pathways to mossy fiber-interneuron plasticity. Interneuron PTP and LTP may provide mechanisms to maintain the balance between synaptic excitation of interneurons and that of principal neurons in the dentate gyrus-CA3 network.

The γ-aminobutyric acid-ergic inhibitory interneurons control the activity of cortical neuronal networks by feedback and feed-forward inhibition (1), synchronize the collective activity of principal neuron ensembles (2), and regulate plasticity at glutamatergic synapses between principal neurons (3). Inhibition mediated by a single interneuron can be very powerful because of the efficacy of interneuron output synapses (4) and the large number of postsynaptic target cells innervated (1).

The strength of interneuron excitation at principal neuron-interneuron synapses is a key factor for maintaining the balance between excitation and inhibition in cortical neuronal networks (5–9). However, the mechanisms that regulate the efficacy of these synapses are not understood. Although recent studies indicated that principal neuron-interneuron synapses are capable of plastic changes in synaptic strength, the direction of plasticity and the possible dependence on interneuron subtype, temperature, brain region, and stimulation paradigm remains highly controversial (10–21).

In the hippocampal mossy fiber system, synapses on interneurons are much more abundant than those on principal cells (22), which further emphasizes the importance of synaptic interneuron excitation and plasticity. At mossy fiber synapses on CA3 pyramidal neurons, a high-frequency stimulation paradigm (HFS) induces various forms of enhancement of synaptic strength, such as posttetanic potentiation (PTP) and long-term potentiation (LTP; ref. 23). In contrast, at mossy fiber synapses on interneurons in the stratum lucidum, HFS causes either little change or long-term depression (LTD; refs. 12 and 15), depending on the subtype of postsynaptic interneuron. It is unknown, however, whether LTP is generally absent in these cells or whether other paradigms are more suitable to induce LTP. Furthermore, it is unclear whether these properties can be extrapolated to other interneuron subtypes in the mossy fiber system.

To address these questions, we examined transmission and plasticity at the granule cell-basket cell synapse in the dentate gyrus by using the paired recording configuration (6). Analysis of unitary excitatory postsynaptic currents (EPSCs) allowed us to distinguish homosynaptic (24, 25) from both heterosynaptic and "passively propagated" forms of plasticity (16) and to determine the locus of expression of long-term changes unequivocally.

Methods

Recording of Unitary and Compound EPSCs. Transverse hippocampal slices (300-μm thickness) were cut from brains of 18–25-day-old Wistar rats by using a vibratome (DTK-1000, Dosaka, Kyoto, Japan). Slices were prepared in ice-cold physiological extracellular solution and then kept submerged in a maintenance chamber at 35°C for 20 min and subsequently at 22–26°C. The recording temperature was 34 ± 2°C. Patch-clamp recordings were obtained under visual control as described (26). Basket cells were identified tentatively by morphological properties and the ability to generate high-frequency trains (>200 Hz) of action potentials (APs) during 500-ms depolarizing current pulses (6, 27). The tentative identification was confirmed in a subset of basket cells (12 of 12) filled with biocytin (0.1%; ref. 6), based on the location of the axonal arborization (1).

Unitary EPSCs were evoked in paired recordings from synaptically connected granule cells and basket cells as described (6). Compound EPSCs were evoked by a glass stimulation pipette (≈1-μm tip diameter) placed in the subgranular portion of the hilar region. Pulses were delivered by using a stimulus isolator and had an amplitude of 1–8 V and a duration of 200 μs. Patch pipettes were pulled from borosilicate glass tubing (2-mm outer diameter, 0.5-mm wall thickness) and had resistances of 1.6–4 MΩ for basket cells and 3.3–8 MΩ for granule cells. Axopatch 200B amplifiers (Axon Instruments, Foster City, CA) were used for current- and voltage-clamp recordings. The stimulation frequency was 0.33 Hz (with the exception of the HFS period). Postsynaptic series resistance was not compensated but was monitored during the experiment by using the amplitude of the capacitive current in response to a 2-mV pulse; the range was 7–15 MΩ. Experiments in which the series resistance increased by >20% were discarded. EPSCs were filtered at 5 kHz by using

This paper was submitted directly (Track II) to the PNAS office.

Abbreviations: HFS, high-frequency stimulation paradigm; PTP, posttetanic potentiation; LTP, long-term potentiation; LTD, long-term depression; EPSC, excitatory postsynaptic current; AP, action potential; aHFS, associative HFS; nHFS, nonassociative HFS; BAPTA, 1,2-bis(2-aminophenoxy)ethane-*N*,*N*,*N*′,*N*′-tetraacetic acid; DCG-4, (2S,2′R,3′R),-2-(2′,3′-dicarboxycyclopropyl)glycine; PDA, phorbol 12,13-diacetate; CV, coefficient of variation; BT, basal transmission; PKA, protein kinase A; PKC, protein kinase C.

*To whom reprint requests should be addressed at: Physiologisches Institut, Universität Freiburg, Hermann-Herder-Strasse 7, D-79104 Freiburg, Germany. E-mail: geigerj@uni-freiburg.de.

The publication costs of this article were defrayed in part by page charge payment. This article must therefore be hereby marked "*advertisement*" in accordance with 18 U.S.C. §1734 solely to indicate this fact.

 www.pnas.org/cgi/doi/10.1073/pnas.251610898

the four-pole low-pass Bessel filter of the amplifier and digitized at 10–20 kHz by using a 1401-plus laboratory interface (CED, Cambridge, UK) interfaced to a PC. The EPC 6.0 software package (CED) was used for stimulus generation and data acquisition. Postsynaptic basket cells were held in the voltage-clamp configuration at −70 mV unless specified differently. Unitary EPSCs had a latency of 0.77 ± 0.05 ms and a 20–80% rise time of 0.29 ± 0.02 ms (12 pairs). Compound EPSCs showed similar latencies and rise times (0.84 ± 0.04 ms and 0.43 ± 0.03 ms, respectively; 11 cells), suggesting that overlapping populations of synapses were stimulated. Both unitary EPSCs (6) and compound EPSCs (6 cells; data not shown) were >95% blocked by 5–10 μM 6-cyano-7-nitroquinoxaline-2,3-dione, indicating that they were mediated mainly by α-amino-3-hydroxy-5-methyl-4-isoxazolepropionic acid receptors.

Paradigms. To test for plasticity at the mossy fiber-basket cell synapse, both associative HFS (aHFS) and nonassociative HFS (nHFS) were applied. The HFS consisted of 12 bursts of stimuli applied at a frequency of 0.33 Hz; each burst was comprised of 25 stimuli applied at a frequency of 30 Hz (see ref. 19). In the aHFS used in paired recordings, HFS of the presynaptic neuron was combined with brief depolarizing suprathreshold current injection into the postsynaptic cell held in current-clamp configuration (with a 0–2-ms delay). In the nHFS in paired recordings, HFS was applied selectively to the presynaptic neuron, and the postsynaptic cell was held in voltage-clamp mode at −70 mV to prevent AP initiation. Finally, in the aHFS used in extracellular mossy fiber stimulation experiments, HFS was delivered to presynaptic axons, and the postsynaptic cell was held in current-clamp configuration. Because compound EPSPs were mostly above threshold for AP generation, this protocol was associative despite the absence of postsynaptic current pulses. In comparison to previous experiments (6), synapses in the present paper showed a smaller apparent release probability (indicated by the larger percentage of failures and the presence of paired-pulse facilitation), presumably because of different slicing and storage conditions implemented here (28). These conditions were chosen to minimize the probability of induction of LTP before recording, e.g., by massive spontaneous activity. Throughout the paper, PTP was measured from EPSCs directly after HFS (0–30 s), and LTP was determined from EPSCs 10–15 min after HFS for unitary EPSCs and 15–20 min after HFS for compound EPSCs (with $t = 0$ at the end of the final HFS). In three compound EPSC recordings that were stable for >30 min, LTP outlasted the time of recording.

Solutions, Chemicals, and Pharmacological Procedures. The physiological extracellular solution contained 125 mM NaCl, 25 mM $NaHCO_3$, 25 mM glucose, 2.5 mM KCl, 1.25 mM NaH_2PO_4, 2 mM $CaCl_2$, and 1 mM $MgCl_2$. For storage of slices, a solution containing 87 mM NaCl, 25 mM $NaHCO_3$, 2.5 mM KCl, 1.25 mM NaH_2PO_4, 0.5 mM $CaCl_2$, 7 mM $MgCl_2$, 25 mM glucose, and 75 mM sucrose was used (28). For paired recording, the intracellular solution (pre- and postsynaptic) contained 120 mM K-gluconate, 20 mM KCl, 0.2 mM EGTA, and 7 mM Na_2-phosphocreatine. For compound EPSC recordings, the intracellular solution contained 135 mM K-gluconate, 20 mM KCl, and 0.1 mM EGTA. The 10 mM 1,2-bis(2-aminophenoxy)ethane-*N*,*N*,*N*′,*N*′-tetraacetic acid (BAPTA) intracellular solution contained 120 mM K-gluconate, 20 mM KCl, and 10 mM BAPTA. The 30 mM BAPTA intracellular solution contained 70 mM K-gluconate, 20 mM KCl, 30 mM BAPTA, and 7 mM Na_2-phosphocreatine. All intracellular solutions contained 2 or 4 mM $MgCl_2$, 4 mM Na_2ATP, or 4 mM K_2ATP, 0.5 mM GTP, and 10 mM Hepes; the pH was adjusted to 7.3 with KOH.

6-Cyano-7-nitroquinoxaline-2,3-dione (CNQX), (2S,2′R,3′R)-2-(2′,3′-dicarboxycyclopropyl)glycine (DCG-4), forskolin, and bisindolylmaleimide I {2-[1-(3-dimethylaminopropyl)indol-3-yl]-3-(indol-3-yl) maleimide} were from Tocris Neuramin (Bristol, UK); phorbol 12,13-diacetate (PDA) was from Research Biochemicals (Natick, MA); H-89 was from Biomol (Plymouth Meeting, PA); and all other chemicals were from Merck, Sigma, Riedel-de-Haën (Seelze, Germany), or Gerbu (Gaiberg, Germany). Forskolin, PDA, H-89, and bisindolylmaleimide were dissolved in dimethyl sulfoxide at concentrations of 100, 1, 40, and 25 mM, respectively, and then added to the bath solution. The concentration of DMSO in the final solution was <0.1%.

When BAPTA was introduced into the postsynaptic cell, >10 min were allowed for the chelator to diffuse to postsynaptic sites before the HFS was applied. Because synapses are located close to the basket cell soma and terminate on dendritic shafts rather than spines (6), this time should be sufficient for BAPTA to diffuse to postsynaptic sites. When H-89 or bisindolylmaleimide were tested, slices were preincubated with the final concentrations of the drugs for >1 h. Both drugs were present also during the experiment. Because the effect of bisindolylmaleimide is less well established than that of H-89, we confirmed that bisindolylmaleimide blocked the effects of PDA (three cells).

Analysis. Unitary EPSCs were analyzed as described (6). The latency of compound EPSCs was measured from the center of the stimulus artifact to the onset of the average EPSC. In summary plots, data points were binned from 10 or 20 consecutive EPSC amplitudes and averaged across experiments. The coefficient of variation (CV) of the peak current was determined from the peak current (including failures) within stationary periods. The paired-pulse ratio was determined as A_2/A_1 of an average trace (from 6 to 25 sweeps; ref. 4). Values are given as the mean ± SEM. Error bars also indicate SEM. The significance of differences was assessed by one-sided Wilcoxon signed rank test (within groups of cells) and by one-sided Wilcoxon rank-sum test (between groups of cells) using the general linear model procedure of SAS 6.12 (SAS Institute, Cary, NC).

Results

We examined glutamatergic synaptic transmission at mossy fiber collateral synapses on γ-aminobutyric acid-ergic interneurons in the dentate gyrus (6). This system allowed us to examine interneuron plasticity in the paired recording configuration (Fig. 1). The application of aHFSs (see *Methods*) resulted in marked changes in the amplitude of unitary EPSCs. The application of a single aHFS induced a marked PTP [to 315% of the basal transmission (BT) value measured within 30 s after aHFS] followed by a significant LTP (to 133% of BT, measured at 10–15 min, eight pairs, $P < 0.05$; Fig. 1 *C* and *D*). The application of a triple aHFS induced similar PTP (319, 388, and 361%, respectively) but substantially greater LTP (187%) in comparison to the single aHFS (three pairs; Fig. 1 *B*, *E*, and *F*). These results demonstrate that homosynaptic PTP and LTP can be induced at single mossy fiber-basket cell synapses, ruling out both heterosynaptic effects and passive propagation in polysynaptic pathways as potential mechanisms (16).

To examine whether an associative paradigm was necessary for LTP induction at this synapse, we further examined the effects of nHFS. A high-frequency stimulation was applied to the presynaptic neuron, and the postsynaptic cell was held in the voltage-clamp configuration at −70 mV. Similar to triple aHFS, triple nHFS induced a marked PTP (299% for the first nHFS). Unlike triple aHFS, however, triple nHFS induced LTD (to 39% of BT, three pairs; Fig. 1*F*) rather than LTP, consistent with previous results (12, 15). Thus spiking of the postsynaptic neuron seems necessary for LTP induction.

To determine the locus of PTP and LTP expression, we examined possible changes in the percentage of failures, CV, and paired-pulse modulation by using paired recordings (Fig. 2).

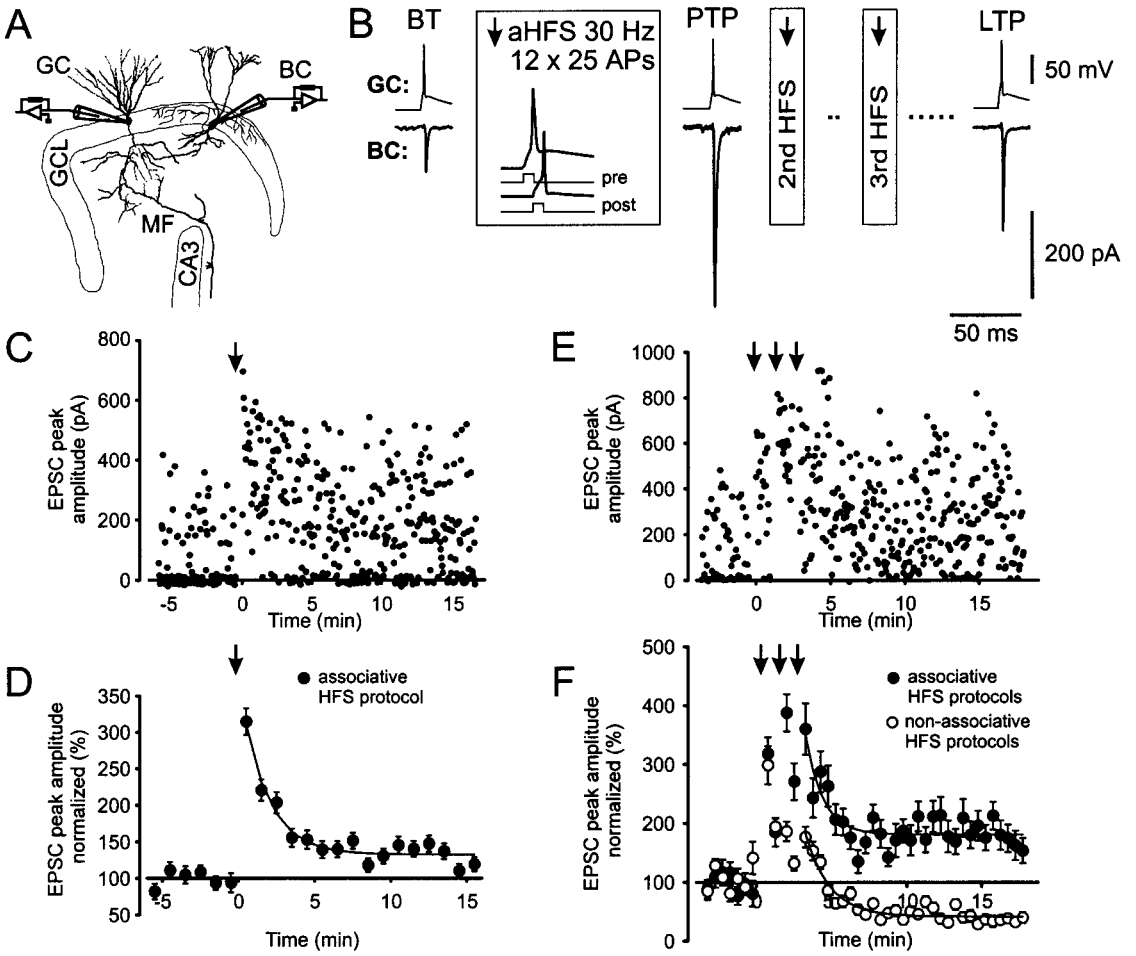

Fig. 1. PTP and LTP of unitary EPSCs at the mossy fiber-basket cell synapse. (*A*) Schematic illustration of the paired recording configuration. GC, granule cell; BC, basket cell; GCL, granule cell layer; CA3, CA3 subfield; MF, mossy fiber. The figure was adapted from ref. 6. (*B*) An aHFS induces both PTP and LTP. Single presynaptic APs are shown on top, and average EPSCs (from 64, 10, and 100 single traces in the time intervals before the first aHFS, directly after the first aHFS, and 10–15 min after the third aHFS, respectively) are depicted below. Boxes indicate details of the aHFSs. (*C* and *D*) PTP and LTP of EPSCs induced by a single aHFS. Unitary EPSC peak amplitudes from paired recordings plotted against time. Data from a single paired recording are shown in *C*, and the summary graph for eight pairs is shown in *D* (with EPSC amplitudes normalized to the control value). The aHFS was applied at $t = 0$, as indicated by the arrow. (*E* and *F*) PTP and LTP of EPSCs induced by triple aHFS. Three single aHFS protocols were separated by 1.5-min intervals. Data from a single paired recording are shown in *E*, and the summary graph for three pairs is shown in *F* (●). For comparison, the effect of triple nHFS with the postsynaptic cell held in the voltage-clamp configuration at −70 mV during induction is depicted also (○, three pairs). The data shown in *B* and *E* were taken from the same experiment. Curves in *D* and *F* represent exponential functions fitted to the data points with time constants of 1.7 (*D*), 3.6 (*F*, aHFS), and 2.4 min (*F*, nHFS). The recording temperature was 34 ± 2°C in these and all subsequent experiments.

After a single aHFS, the percentage of failures decreased significantly from 47 ± 6% in BT to 17 ± 5% during PTP and 25 ± 6% during LTP ($P < 0.05$ in both conditions; Fig. 2*A*, filled bars, left). Furthermore, a plot of the CV^{-2} against the mean EPSC peak amplitude in the LTP phase, both normalized to the respective BT values (29), revealed that the data points were located close to the identity line (Fig. 2*B*). Finally, the ratio of EPSC amplitudes evoked by pairs of presynaptic APs, separated by 20-ms intervals, was changed by a single aHFS (Fig. 2*C*). The mean paired-pulse ratio decreased from 1.80 ± 0.11 in BT to 1.34 ± 0.31 during PTP and to 1.30 ± 0.18 during LTP (Fig. 2*D*, filled bars, left). Qualitatively similar results were obtained for LTP induced by triple aHFS, although the extent of the effect appeared to be larger (Fig. 2 *A* and *D*, filled bars, center; Fig. 2*B*). In contrast, reverse effects were observed for LTD after triple nHFS (Fig. 2 *A* and *D*, open bars, right; Fig. 2*B*), consistent with previous results for interneuron LTD (14, 15). Collectively, these results indicate that PTP and LTP/LTD at the mossy fiber-basket cell synapse are expressed at presynaptic sites.

To study the mechanisms of induction and expression of PTP and LTP, we examined compound EPSCs in basket cells evoked by extracellular mossy fiber stimulation, which gave higher long-term stability and larger peak current amplitudes than single inputs (Fig. 3). Both, unitary and compound EPSCs were depressed after bath application of the group 2 metabotropic glutamate receptor agonist DCG-4 (four pairs and seven cells, respectively; Fig. 3 *A* and *B*), confirming that they were generated by mossy fiber synapses (30). An aHFS induced a marked PTP followed by significant LTP of compound EPSC peak amplitudes. On average, the PTP was 303%, and the LTP (measured 15–20 min after the aHFS protocol) was 127% of the control value before aHFS (11 cells; $P < 0.05$; Fig. 3 *C* and *D*, filled circles). Thus PTP and LTP were similar to those observed in paired recordings (with low postsynaptic EGTA concentration in both sets of experiments).

LTP induction at glutamatergic synapses requires a rise in postsynaptic Ca^{2+} concentration (31–33). We therefore tested whether the Ca^{2+} chelator BAPTA was able to suppress the

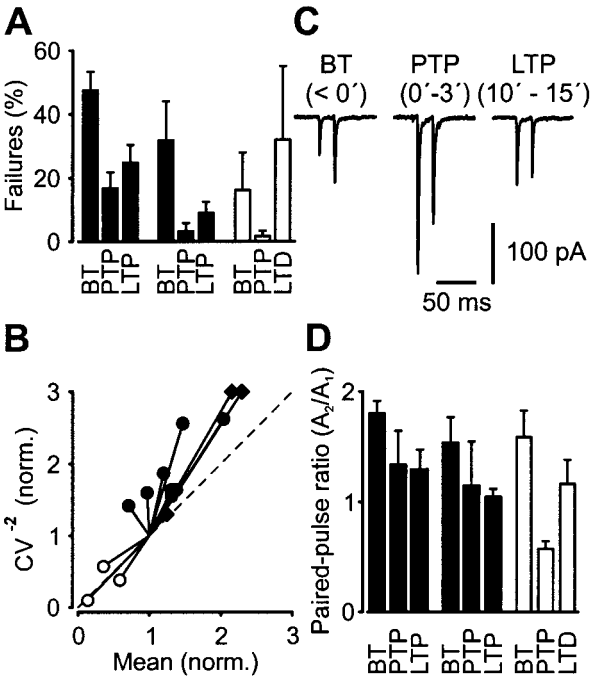

Fig. 2. Presynaptic locus of PTP and LTP of unitary EPSCs at the mossy fiber-basket cell synapse. (*A*) Bar graph of the percentage of failures during BT, PTP, and LTP/LTD (with time intervals identical to those specified in Fig. 1). The mean effects of single aHFS (filled bars, left), triple aHFS (filled bars, center), and triple nHFS (open bars, right). (*B*) CV analysis of long-term changes. The CV^{-2} of the EPSC amplitude in the late phase after induction was plotted against mean, both normalized to their respective control values before HFS. The effects of single aHFS (●), triple aHFS (♦), and triple nHFS (○) are shown. The location of the data points with respect to the identity line (dashed) was consistent with presynaptic changes in all cases. (*C*) Average unitary EPSCs (from 25, 15, and 25 single traces during BT, PTP, and LTP phases, respectively; single aHFS protocol) evoked by pairs of two APs, separated by 20-ms intervals. (*D*) Paired-pulse ratios for BT, PTP, and LTP/LTD periods. The mean effects of single aHFS (filled bars, left), triple aHFS (filled bars, center), and triple nHFS (open bars, right) are shown. The paired-pulse ratio was determined as A_2/A_1 from average trace.

induction of LTP at mossy fiber-basket cell synapses (Fig. 3 *C–F*). Neither 10 nor 30 mM intracellular BAPTA affected PTP (Fig. 3*E*). Intracellular BAPTA (10 mM), which blocks LTP dependent on *N*-methyl-D-aspartate receptors and Ca^{2+}-permeable L-α-amino-3-hydroxy-5-methyl-4-isoxazolepropionate-type glutamate receptors (19), had no significant effect on LTP (143%; $P = 0.4$; Fig. 3 *C* and *F*). However, 30 mM intracellular BAPTA, which is required to block some forms of *N*-methyl-D-aspartate receptor-independent LTP at the mossy fiber-CA3 pyramidal neuron synapse (34), resulted in a significant attenuation of LTP (107%; $P < 0.05$; Fig. 3 *D* and *F*). This result is corroborated by the cumulative distributions of both PTP and LTP in individual experiments (Fig. 3 *E* and *F*). These results suggest that induction of LTP at the mossy fiber-basket cell synapse is only weakly sensitive to intracellular BAPTA, which is reminiscent of a previous report of the mossy fiber-CA3 pyramidal neuron synapse (35).

At the mossy fiber synapse on CA3 pyramidal neurons, both protein kinase A (PKA) and protein kinase C pathways are thought to play key roles in long-term enhancement of synaptic strength (36–38). We therefore investigated whether activation of adenylyl cyclase or PKC was able to mimic the induction of LTP (Fig. 4). Bath application of either 50 μM forskolin for 5 min or 1 μM PDA for 25 min resulted in a persistent increase in the amplitude of the compound EPSC (Fig. 4 *A* and *B*). The mean potentiation by forskolin, measured 20–25 min after the onset of the forskolin application, was 239%, and that by PDA, measured 28–33 min after the onset, was 217%. CV analysis indicated that both forskolin- and PDA-induced potentiation were expressed at a presynaptic site (Fig. 4*B*), similar to aHFS-induced LTP.

To examine whether PKA and PKC pathways were involved in the induction or expression of plasticity, aHFS was performed in the presence of the PKA blocker H-89 (10 μM) or the PKC blocker bisindolylmaleimide (1 μM). Both H-89 and bisindolylmaleimide, present continuously for >1 h before the onset of recording, decreased the extent of PTP in comparison to the control experiments. In the presence of H-89 or bisindolylmaleimide, the amount of PTP was reduced significantly to 196 and 194% of BT, respectively ($P < 0.05$ in both conditions). In contrast, the effect on LTP was differential. In the presence of H-89, LTP was 129% (not significantly different from control experiments, $P = 0.46$). In the presence of bisindolylmaleimide, however, LTP was reduced significantly (102%; $P < 0.05$). This result is shown also in the cumulative distributions of both PTP and LTP in individual experiments in the presence of H-89 or bisindolylmaleimide (Fig. 4 *E* and *F*).

Discussion

Paired recordings at physiological temperature revealed that both short- and long-term forms of homosynaptic plasticity coexist at the mossy fiber-basket cell synapse in the dentate gyrus. Together with recent reports of LTP in interneurons in the hippocampal CA1 region (20, 21), the present data change the prevailing view of static synaptic transmission at principal neuron-interneuron synapses (16). For PTP at the mossy fiber-basket cell synapse, the amount of potentiation is independent of the induction paradigm (aHFS versus nHFS) and is completely insensitive to 30 mM intracellular BAPTA, indicating a presynaptic site of induction. Furthermore, analysis of the failures and paired-pulse ratio indicates a presynaptic locus of expression, implying that PTP is entirely presynaptic. Finally, PKA and PKC, with presumably presynaptic localization, seem necessary for maximal PTP. For LTP at the mossy fiber-basket cell synapse, a different model emerges. Both the requirement for an associative paradigm and the attenuation by 30 mM BAPTA may suggest a postsynaptic site of induction of LTP. In contrast, the analysis of failures, CV, and the paired-pulse ratio indicates a presynaptic locus of expression, implying some form of retrograde signaling (39, 40). PKC (but not PKA) appears to be involved in LTP induction, although its exact location remains unknown.

In comparison to the mossy fiber-pyramidal neuron synapse in the CA3 region, both similarities and differences emerge. First, the phenomenology of PTP (41) and LTP (23, 35, 42–45) and the homosynaptic nature of plasticity (24, 25) at the mossy fiber-pyramidal neuron synapse are very similar to those reported here. The locus and mechanisms of induction of LTP at the synapse on CA3 pyramidal neurons are controversial, especially with respect to the possible coexistence of Hebbian and non-Hebbian forms of plasticity and the role of postsynaptic Ca^{2+} (23, 35, 44, 46); it therefore is difficult to make direct comparisons to our results. Nevertheless, a marked difference is that both aHFS and nHFS induce LTP at the synapse on pyramidal neurons (23, 35, 44), whereas these paradigms change synaptic strength in different directions at the synapse on basket cells. Finally, the expression of LTP at the mossy fiber-pyramidal neuron synapse is also presynaptic (47). The chemical potentiation by forskolin and phorbol ester is almost identical (45, 48), but the involvement of the PKA and PKC pathways in plasticity appears to be distinct. PKA is essential for LTP induction at the

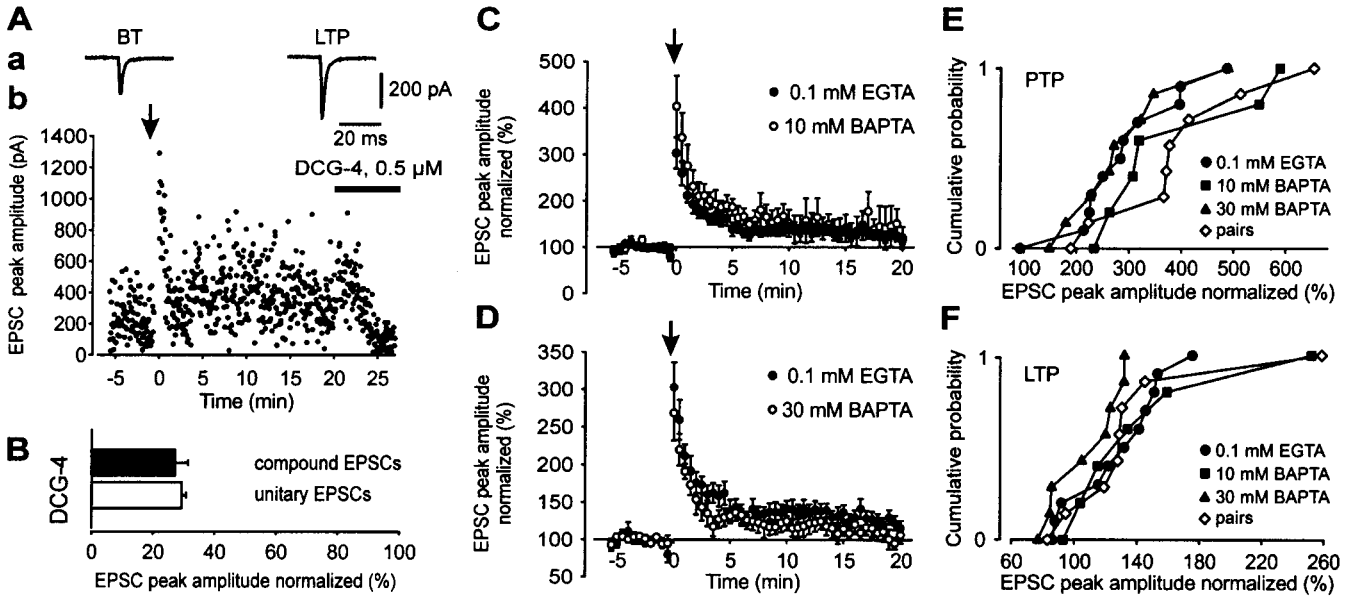

Fig. 3. The aHFS-induced LTP of compound EPSCs shows weak sensitivity to the Ca^{2+} chelator BAPTA. (*A*) Compound EPSCs are similar to unitary EPSCs with respect to PTP, LTP after aHFS, and DCG-4 sensitivity. *Aa*, average compound EPSCs in BT and LTP phases (stimulus artifacts blanked); *Ab*, corresponding EPSC peak amplitude values plotted against time. (*B*) Bar graph of compound EPSC amplitude (filled) and unitary EPSC amplitude (open) in the presence of 0.5–1 μM DCG-4 relative to respective control values. (*C* and *D*) Effects of single aHFS on compound EPSC amplitude with 0.1 mM intracellular EGTA (●; 11 cells), 10 mM intracellular BAPTA (*C*, ○; six cells), and 30 mM BAPTA (*D*, ○; eight cells). Amplitudes were normalized to the mean EPSC peak amplitude before aHFS. The aHFS was applied at $t = 0$, as indicated by the arrow. (*E* and *F*) Cumulative distributions of the extent of aHFS-induced PTP (*E*) and LTP (*F*) of compound EPSCs in individual experiments in 0.1 mM internal EGTA, 10 mM BAPTA, and 30 mM BAPTA. Paired recording data (with 0.2 mM internal EGTA) are shown superimposed.

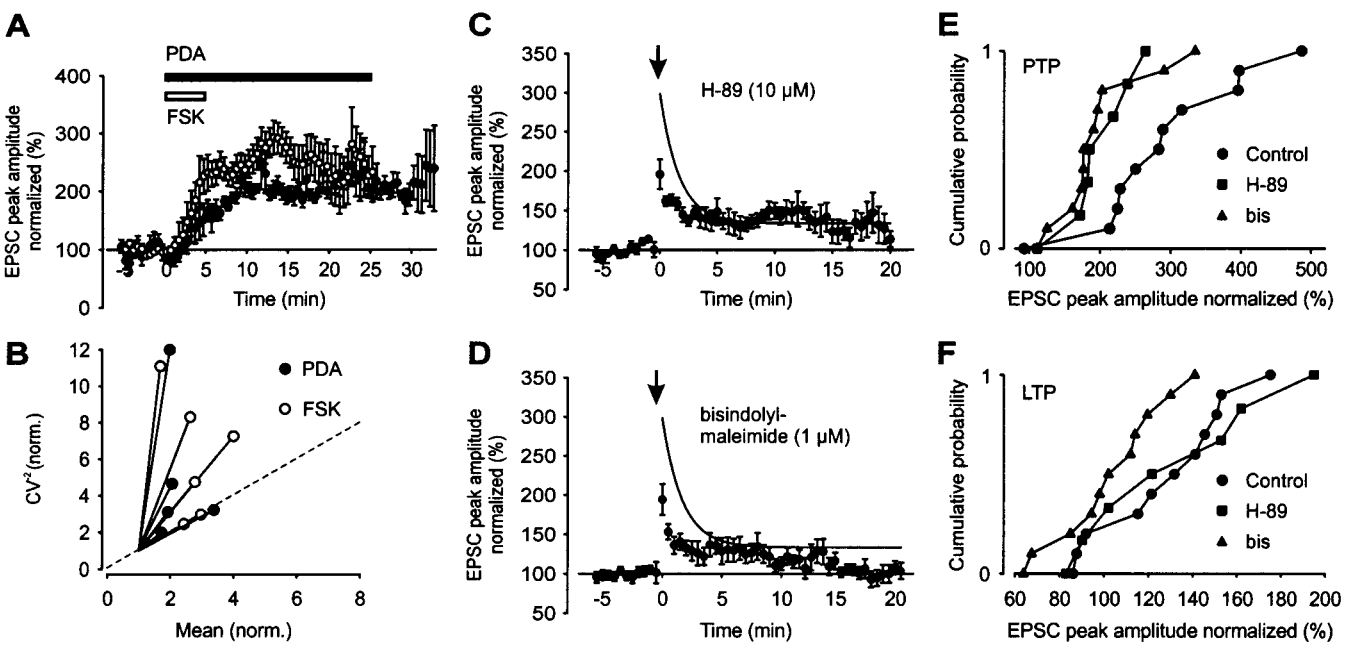

Fig. 4. Involvement of PKA and PKC pathways in aHFS-induced PTP and LTP of compound EPSCs. (*A*) Potentiation of compound EPSC amplitude (normalized to BT period) by bath application of 50 μM forskolin (○; six cells) and 1 μM PDA (●; five cells; horizontal bars indicate application times). (*B*) CV analysis of forskolin- (○) and PDA- (●) induced potentiation. The CV^{-2} of the EPSC amplitude 10–15 min (forskolin, two cells), 15–20 min (forskolin, four cells; PDA, one cell), and 20–25 min (PDA, four cells) after the onset of application was plotted against mean, both normalized to their respective control values. Location of the data points with respect to the identity line (dashed) suggests presynaptic changes. (*C* and *D*) Effects of single aHFS on compound EPSC amplitude after preincubation with 10 μM H-89 (*C*, seven cells) and 1 μM bisindolylmaleimide (*D*, 11 cells). The aHFS was applied at $t = 0$, as indicated by the arrow. Curves in *C* and *D* represent exponential function fitted to the control data points (0.1 mM EGTA) in Fig. 3 *C* and *D* (●; time constant 1.7 min). (*E* and *F*) Cumulative distributions of the extent of aHFS-induced PTP (*E*) and LTP (*F*) of compound EPSCs in individual experiments in control conditions (same experiments as shown in Fig. 3*C*), after preincubation with 10 μM H-89 (*C*), and one after preincubation with 1 μM bisindolylmaleimide (*D*).

synapse on pyramidal neurons (36, 45), whereas PKC is necessary for LTP induction at the synapse on basket cells.

In comparison to mossy fiber synapses on other interneurons, differences are more apparent than similarities. First, the phenomenology of synaptic plasticity is entirely different at mossy fiber-stratum lucidum (SL) interneuron synapses in the CA3 region. Neither PTP nor LTP was observed in the mossy fiber-SL interneuron synapse (12, 15). In contrast, nHFS induces LTD in a subset of cells (15). Whether aHFS or other paradigms induce PTP or LTP in SL interneurons remains to be addressed. However, even if paradigms inducing potentiation at mossy fiber-SL interneuron synapses do exist, the lack of forskolin effects on synaptic strength (12) would suggest that distinct intracellular signaling cascades have to be involved. Thus, there seem to be major target cell-specific differences between subtypes of mossy fiber synapses.

Because interneurons are major targets of the mossy fiber pathway (22), PTP and LTP at mossy fiber-interneuron synapses will have profound implications for the signal flow in the hippocampal input region. A potentiation in synaptic strength at mossy fiber-basket cell synapses will increase feedback inhibition because the large impact of both input and output synapses of basket cells (4, 6) and the high level of connectivity (1, 22). This functional property may promote a sparse and efficient coding of information in the dentate gyrus-CA3 network (49).

We thank Drs. J. Bischofberger and M. Martina for critically reading an earlier version of the manuscript and A. Blomenkamp for excellent technical assistance. Supported by the Deutsche Forschungsgemeinschaft Sonderforschungsbereich 505/C5 and Human Frontiers Science Program Organization Grant RG0017/98.

1. Freund, T. F. & Buzsáki, G. (1996) *Hippocampus* **6,** 347–470.
2. Cobb, S. R., Buhl, E. H., Halasy, K., Paulsen, O. & Somogyi, P. (1995) *Nature (London)* **378,** 75–78.
3. Davies, C. H., Starkey, S. J., Pozza, M. F. & Collingridge, G. L. (1991) *Nature (London)* **349,** 609–611.
4. Kraushaar, U. & Jonas, P. (2000) *J. Neurosci.* **20,** 5594–5607.
5. Miles, R. (1990) *J. Physiol. (London)* **428,** 61–77.
6. Geiger, J. R. P., Lübke, J., Roth, A., Frotscher, M. & Jonas, P. (1997) *Neuron* **18,** 1009–1023.
7. Geiger, J. R. P., Roth, A., Taskin, B. & Jonas, P. (1999) in *Ionotropic Glutamate Receptors in the CNS, Handbook of Experimental Pharmacology* **141,** eds. Jonas, P. & Monyer, H. (Springer, Berlin), pp. 363–398.
8. Ali, A. B., Deuchars, J., Pawelzik, H. & Thomson, A. M. (1998) *J. Physiol. (London)* **507,** 201–217.
9. Buhl, E. H., Tamás, G., Szilágyi, T., Stricker, C., Paulsen, O. & Somogyi, P. (1997) *J. Physiol. (London)* **500,** 689–713.
10. Maccaferri, G. & McBain, C. J. (1995) *Neuron* **15,** 137–145.
11. Maccaferri, G. & McBain, C. J. (1996) *J. Neurosci.* **16,** 5334–5343.
12. Maccaferri, G., Tóth, K. & McBain, C. J. (1998) *Science* **279,** 1368–1370.
13. McMahon, L. L. & Kauer, J. A. (1997) *Neuron* **18,** 295–305.
14. Laezza, F., Doherty, J. J. & Dingledine, R. (1999) *Science* **285,** 1411–1414.
15. Toth, K., Suares, G., Lawrence, J. J., Philips-Tansey, E. & McBain, C. J. (2000) *J. Neurosci.* **20,** 8279–8289.
16. McBain, C. J., Freund, T. F. & Mody, I. (1999) *Trends Neurosci.* **22,** 228–235.
17. Ouardouz, M. & Lacaille, J.-C. (1995) *J. Neurophysiol.* **73,** 810–819.
18. Cowan, A. I., Stricker, C., Reece, L. J. & Redman, S. J. (1998) *J. Neurophysiol.* **79,** 13–20.
19. Mahanty, N. K. & Sah, P. (1998) *Nature (London)* **394,** 683–687.
20. Christie, B. R., Franks, K. M., Seamans, J. K., Saga, K. & Sejnowski, T. J. (2000) *Hippocampus* **10,** 673–683.
21. Perez, Y., Morin, F. & Lacaille, J.-C. (2001) *Proc. Natl. Acad. Sci. USA* **98,** 9401–9406. (First Published July 10, 2001; 10.1073/pnas.161493498)
22. Acsády, L., Kamondi, A., Sík, A., Freund, T. & Buzsáki, G. (1998) *J. Neurosci.* **18,** 3386–3403.
23. Zalutsky, R. A. & Nicoll, R. A. (1990) *Science* **248,** 1619–1624.
24. Lopez-Garcia, J. C., Arancio, O., Kandel, E. R. & Baranes, D. (1996) *Proc. Natl. Acad. Sci. USA* **93,** 4712–4717.
25. Tong, G., Malenka, R. C. & Nicoll, R. A. (1996) *Neuron* **16,** 1147–1157.
26. Stuart, G. J., Dodt, H.-U. & Sakmann, B. (1993) *Pflügers Arch.* **423,** 511–518.
27. Koh, D.-S., Geiger, J. R. P., Jonas, P. & Sakmann, B. (1995) *J. Physiol. (London)* **485,** 383–402.
28. Geiger, J. R. P. & Jonas, P. (2000) *Neuron* **28,** 927–939.
29. Malinow, R. & Tsien, R. W. (1990) *Nature (London)* **346,** 177–180.
30. Kamiya, H., Shinozaki, H. & Yamamoto, C. (1996) *J. Physiol. (London)* **493,** 447–455.
31. Bliss, T. V. P. & Collingridge, G. L. (1993) *Nature (London)* **361,** 31–39.
32. Lynch, G., Larson, J., Kelso, S., Barrionuevo, G. & Schottler, F. (1983) *Nature (London)* **305,** 719–721.
33. Collingridge, G. L., Kehl, S. J. & McLennan, H. (1983) *J. Physiol. (London)* **334,** 33–46.
34. Kapur, A., Yeckel, M., Gray, R. & Johnston, D. (1998) *J. Neurophysiol.* **79,** 2181–2190.
35. Yeckel, M. F., Kapur, A. & Johnston, D. (1999) *Nat. Neurosci.* **2,** 625–633.
36. Huang, Y.-Y., Li, X.-C. & Kandel, E. R. (1994) *Cell* **79,** 69–79.
37. Weisskopf, M. G., Castillo, P. E., Zalutsky, R. A. & Nicoll, R. A. (1994) *Science* **265,** 1878–1882.
38. Son, H. & Carpenter, D. O. (1996) *Neuroscience* **72,** 1–13.
39. Stevens, C. F. (1993) *Cell* 72, Suppl., 55–63.
40. Zilberter, Y., Kaiser, K. M. M. & Sakmann, B. (1999) *Neuron* **24,** 979–988.
41. Griffith, W. H. (1990) *J. Neurophysiol.* **63,** 491–501.
42. Kobayashi, K., Manabe, T. & Takahashi, T. (1996) *Science* **273,** 648–650.
43. Derrick, B. E. & Martinez, J. L., Jr. (1996) *Nature (London)* **381,** 429–434.
44. Urban, N. N. & Barrionuevo, G. (1996) *J. Neurosci.* **16,** 4293–4299.
45. Weisskopf, M. G. & Nicoll, R. A. (1995) *Nature (London)* **376,** 256–259.
46. Mellor, J. & Nicoll, R. A. (2001) *Nat. Neurosci.* **4,** 125–126.
47. Xiang, Z., Greenwood, A. C., Kairiss, E. W. & Brown, T. H. (1994) *J. Neurophysiol.* **71,** 2552–2556.
48. Kamiya, H. & Yamamoto, C. (1997) *Neuroscience* **80,** 89–94.
49. Treves, A. & Rolls, E. T. (1992) *Hippocampus* **2,** 189–199.